

리튬과 소듐이 층간삽입된 FeMoO_4Cl 의 전기화학적 성질

張舜浩[§] · 宋丞婉 · 崔珍禧*

[§]한국전자통신연구소 반도체연구단

*서울대학교 자연과학대학 화학과

(1997. 7. 1 접수)

Electrochemical Aspects of Lithium and Sodium Intercalation into Two Dimensional FeMoO_4Cl

Soon-Ho Chang[§], Seung-Wan Song, and Jin-Ho Choy*

[§]Electronics and Telecommunications Research Institute, Taejeon, 305-600, Korea

*Department of Chemistry, College of Natural Sciences, Seoul National University, 151-742, Seoul, Korea

(Received July 1, 1997)

요약. 리튬 이온과 소듐 이온을 전기화학적, 화학적인 방법으로 2차원 층상구조의 FeMoO_4Cl 에 층간 삽입시켰다. FeMoO_4Cl 에 대한 충방전 곡선에서 넓은 고용체 영역이 관찰되는데, 알칼리 금속이 층간삽입되므로써 발생하는 단위세포 크기의 변화와 전자의 국부화 현상으로 인한 것이다. 리튬이 층간삽입된 경우, $\text{Li}_x\text{FeMoO}_4\text{Cl}$ 조성 근처에서 좁은 $\text{Li}_x\text{FeMoO}_4\text{Cl}$ ($0.95 \leq x \leq 1.06$) 고용체 영역이 형성된다. Armand 모델을 이용하여 OCV 곡선 fitting을 수행한 결과, 리튬의 층간삽입에 따른 충방전 곡선의 변화는 층간삽입 과정에서 일어나는 이 물질의 전자적, 구조적 변화에 의한 것임을 알 수 있었다.

ABSTRACT. Lithium and sodium ions have been intercalated into two dimensional structure of FeMoO_4Cl . The electronic localization and the large difference in unit cell parameter between the pristine material and the intercalates lead to the existence of large biphased domains. In the case of the lithium system, a narrow range of $\text{Li}_x\text{FeMoO}_4\text{Cl}$ ($0.95 \leq x \leq 1.06$) solid solution has been found around the $\text{LiFeMoO}_4\text{Cl}$ composition. The OCV curve fitting has been performed using Armand's model. The occurrence of several parts in the charge-discharge curve is related to the electronic and structural modifications of the material during the intercalation process.

INTRODUCTION

In previous papers we have demonstrated that FeMO_4Cl ($M=\text{Mo}, \text{W}$) is a host structure for both lithium and amine intercalations.¹⁻⁴ The triangular faces of the FeO_4Cl square pyramid, being negatively charged, can interact with cations like Li^+ , while the square face which is positively charged due to the proximity of the iron ion, is able to interact with negative dipolar species like amine to form an octahedral environment for the iron atom. From this structural point of view, the framework of FeMoO_4Cl exhibits a strong 2D character due to the linking of FeO_4Cl square pyramids by MoO_4 tetrahedra (Fig. 1) in the xy plane. Nevertheless,

from a magnetic point of view, this material can be considered as being in the border between 1D and 2D as a result of the $\text{ClOFe} \cdots \text{ClOFe}$ bonding which takes place perpendicularly to the layers.^{5,6} In the previous paper, the chemically prepared $\text{LiFeMoO}_4\text{Cl}$ has been characterized magnetically^{1,7} and by XPS.^{8,9} Both experiments show that only iron is reduced during the lithium intercalation. Furthermore, the intercalation of lithium between the layers leads to a strong decrease in the interlayer spacing which reduces the structural anisotropy.^{2,7}

In the present work, lithium and sodium ions were intercalated into FeMoO_4Cl and the elec-

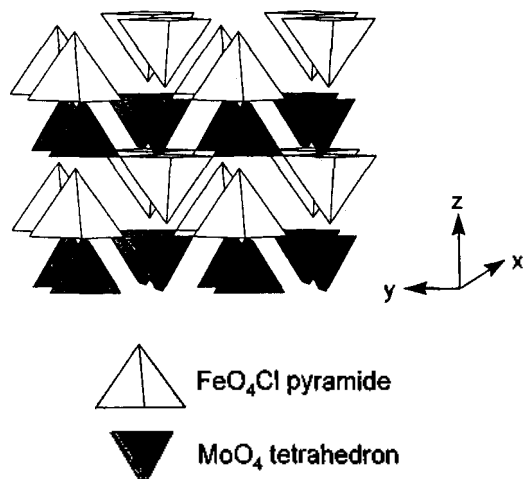


Fig. 1. Schematic representation of the polyhedra linking in the FeMoO_4Cl structure.

trochemical properties for the intercalates have been studied to identify the relationship between structural change and electrochemical behavior by means of charge-discharge experiment and OCV curve fitting.

EXPERIMENTAL

FeMoO_4Cl has been prepared by chemical vapor transport from Fe_2O_3 , MoO_3 and FeCl_3 as previously reported.¹ Electrochemical lithium intercalation was carried out in lithium cells using a lithium foil as negative plate, a 1 M solution of LiClO_4 in PC as electrolyte and a mixture of the positive electrode material and Ketjen black as positive electrode. Such electrochemical cells were realized either with FeMoO_4Cl or $\text{LiFeMoO}_4\text{Cl}$. The latter was chemically obtained by the reaction of LiI on FeMoO_4Cl in CH_3CN . All materials were characterized by powder X-ray diffraction with Ni-filtered $\text{Cu K}\alpha$ radiation.

RESULTS AND DISCUSSION

Lithium intercalation

Electrochemical intercalation. Fig. 2 shows the variation of cell voltage vs lithium amount (x) for two cells discharged at two different current densities of 100 and 30 $\mu\text{A}/\text{cm}^2$, respectively. A

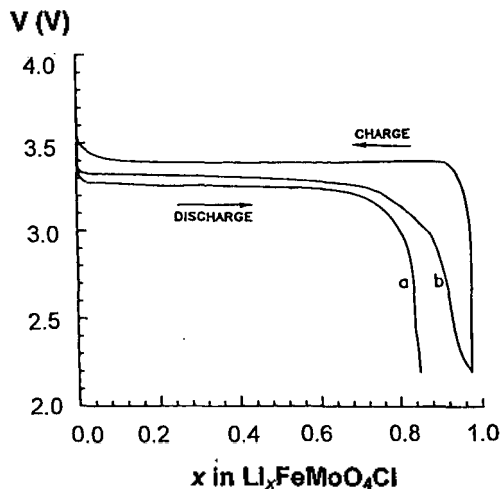


Fig. 2. Variation of the $\text{Li}/\text{FeMoO}_4\text{Cl}$ cell voltage in a discharge process with the constant current density of (a) 100 $\mu\text{A}/\text{cm}^2$ and (b) 30 $\mu\text{A}/\text{cm}^2$.

small difference between two discharge curves shows that the polarization is small, indicating that the intercalation kinetics is rapid. Moreover, about 90% of the capacity is recovered if the cell is discharged at 100 $\mu\text{A}/\text{cm}^2$. The curve shape is characteristic of the existence of a large biphased domain between FeMoO_4Cl and $\text{LiFeMoO}_4\text{Cl}$. The existence of this two phase domain is confirmed by the X-ray diffraction study for the electrode materials recovered at various degrees of intercalation. Moreover, as shown in Fig. 2, the intercalation process is completely reversible. A small cell voltage difference between charge and discharge curves emphasizes again that the polarization is small.

Fig. 3 shows the electrochemical behavior of a $\text{Li}/\text{FeMoO}_4\text{Cl}$ cell after a deep discharge down to 1.2 V vs Li. In these conditions, the $\text{Li}_3\text{FeMoO}_4\text{Cl}$ composition can be reached. Although the shape of the charge curve is completely different from that of the first discharge, the 2nd discharge exhibits a strong similarity with the first one. Nevertheless, it should be noted that the extent of the first plateau is considerably reduced. At the second charge, the curve becomes more monotonous. Such a behavior generally characterizes an amorphization of the material. In order to illustrate this behavior, the X-ray diffraction patterns for FeMo

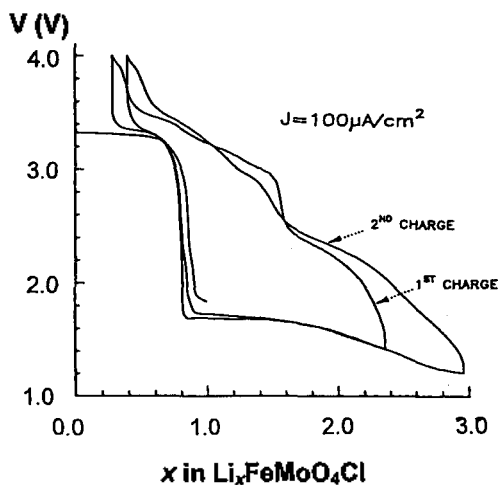


Fig. 3. Cycling behavior of the Li/FeMoO₄Cl cell with a deep discharge.

O₄Cl and the intercalates (LiFeMoO₄Cl and Li₃FeMoO₄Cl) are shown in Fig. 4, indicating the topotactic character of lithium intercalation reaction. The main difference between the pristine and two intercalates results from a decrease in symmetry from tetragonal to monoclinic.^{1,2,7-9} After a deep discharge, only the (001) line ($2\theta=17^\circ$), corresponding to the interlayer spacing, remains, where the broadening of all the other peaks shows the amorphization of the material due to the reduction of hexavalent molybdenum. Since three lithium ions are intercalated to form Li₃FeMoO₄Cl, it could be assumed that in this material the iron and the molybdenum are in the divalent and the tetra-

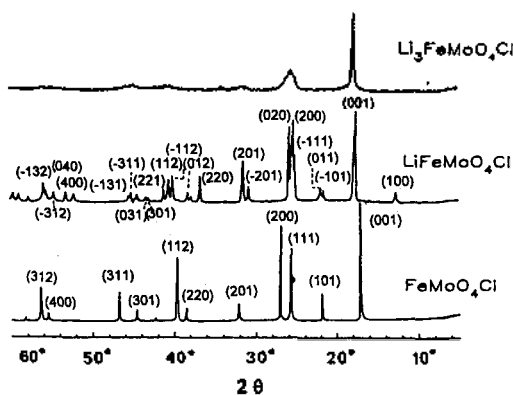


Fig. 4. Modifications of the powder X-ray diffraction pattern depending on the intercalation rate.

valent states, respectively.

Chemical intercalation. According to Torardi *et al.*,⁷ as the voltage of the first plateau is higher than the I⁰/I redox couple potential, LiI can be used as the reducing reagent to intercalate lithium into the FeMoO₄Cl lattice. LiFeMoO₄Cl in the present work has been prepared in this way in order to study the electrochemical behavior in the vicinity of this composition. The X-ray diffraction patterns of LiFeMoO₄Cl obtained by both techniques (chemical and electrochemical) are identical and consistent with that previously reported.⁷

The intercalation with n-butyl lithium has also been tried. As it is well known, this reaction leads to a deeply reduced phase, even if a small amount of n-butyl lithium is used. With an excess of n-butyl lithium, a Li_xFeMoO₄Cl phase ($x>3$) is obtained. Its X-ray diffraction pattern is characteristic of an amorphous phase. Moreover, the diffraction line associated with the interslab spacing ($2\theta=17^\circ$) that was observed for the electrochemically prepared Li₃FeMoO₄Cl (Fig. 4) has disappeared in this case. In fact the reducing character of n-butyl lithium is so strong that the structure is completely destroyed. This result emphasizes a quite general behavior of chemical intercalation using n-butyl lithium in oxides. Bringing the material in contact with n-butyl lithium solution is equivalent to performing a potentiostatic discharge for a Li cell down to 1 V, practically without current limitation. Since the oxides generally exhibit quite high potentials vs Li (3 to 4 V), the reduction reaction leads to such a high degree of intercalation that the process is often no longer reversible. Moreover, the very high reactivity of n-butyl lithium in chemical intercalation makes it very far from equilibrium, so that the relaxation by mechanical constraint is much more difficult than in electrochemical experiments which are generally close to equilibrium. As a consequence, the structure of the chemically intercalated material is often rather disorganized.

Sodium intercalation

Sodium can be intercalated in FeMoO₄Cl either chemically or electrochemically. As in the case of LiFeMoO₄Cl,⁷ NaFeMoO₄Cl can be obtained by

the reaction of NaI in solution of CH_3CN on FeMoO_4Cl . In fact, this reaction seems to be more complex since NaCl is always observed as a side product mixed with $\text{NaFeMoO}_4\text{Cl}$. This might result from a partial decomposition of the material or from a I^-/Cl^- exchange reaction. Another point concerns the very slow sodium intercalation kinetics. The reaction with NaI requires about 20 days while in the case of the lithium system, 3 days are enough to obtain pure $\text{LiFeMoO}_4\text{Cl}$ by the reaction of LiI on FeMoO_4Cl .

The electrochemical intercalation of sodium in FeMoO_4Cl is very difficult as shown in Fig. 5. The voltage vs sodium content curve is characteristic of the existence of a two phase domain for the smallest sodium amounts. For the range with $x > 0.4$, the voltage drops rapidly. The powder X-ray diffraction study for the materials recovered after intercalation and OCV experiments shows that in the composition range from 0.0 to 1.0 a two phase domain is observed. Therefore the strong voltage decrease emphasizes a material polarization resulting from the difficulty for Na^+ ions to move in the $\text{NaFeMoO}_4\text{Cl}$ framework.

Structural comparison of $\text{LiFeMoO}_4\text{Cl}$ and $\text{NaFeMoO}_4\text{Cl}$ phases

The unit cell parameters of Li and Na in-

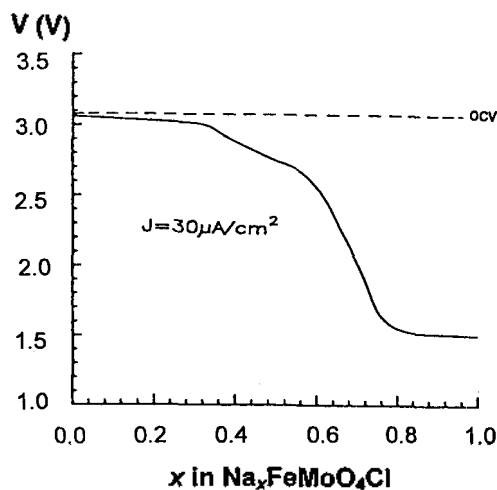


Fig. 5. Electrochemical behavior of the Na/ FeMoO_4Cl cell, (—) continuous discharge at $30 \mu\text{A}/\text{cm}^2$ and (---) OCV curve.

Table 1. Variation in the lattice parameters for FeMoO_4Cl , $\text{LiFeMoO}_4\text{Cl}$ and $\text{NaFeMoO}_4\text{Cl}$

Compound	a(Å)	b(Å)	c(Å)	β (deg)	cell volume (Å ³)
FeMoO_4Cl	6.668	6.668	5.223	90.0	232.2
$\text{LiFeMoO}_4\text{Cl}$	7.010	6.910	5.030	91.3	243.6
$\text{NaFeMoO}_4\text{Cl}$	7.170	7.180	5.182	90.0	266.8

tercalates are present in Table 1. The increase in cell volume results from the steric effect not only due to the alkali metal intercalation but also due to the larger size of Fe^{2+} ions compared to Fe^{3+} ones. While the a and b parameters increase from FeMoO_4Cl to $\text{LiFeMoO}_4\text{Cl}$ and $\text{NaFeMoO}_4\text{Cl}$, a strong decrease in the c parameter (which is equal to the interslab distance) upon intercalation is observed.

In the intercalated phases, the Fe-Cl bond lengths within the FeMoO_4Cl layer and between the adjacent ones become nearly equal to 2.528 Å and 2.493 Å, respectively, for $\text{LiFeMoO}_4\text{Cl}$, which leads to an octahedral environment for iron and therefore to a 3D character.^{8,9} This point will be discussed in the next part from the electrochemical view point. As presented in Fig. 6, the Li^+ ions are situated between two faces of FeO_4Cl_2 octahedra belonging to adjacent FeMoO_4Cl sheets. This linking entails the strong decrease in the c parameter (Table 1) compared to the pristine. Even in the case of $\text{NaFeMoO}_4\text{Cl}$ the c parameter decreases upon intercalation, which explains why the Na^+ diffusion is so difficult in $\text{NaFeMoO}_4\text{Cl}$.

The relation between the shape of thermodynamic electrochemical curves and structure

The potential variation for an intercalation electrode can be described according to Armand's model, considering the alkali metal intercalation as the formation of a solution of Li^+ ions and electrons within the host structure.¹⁰

The potential variation (E) vs the site occupancy y ($y = x/x_{\text{max}}$) is given by the following formula;

$$E = E_0 - (nRT/F) \ln[y/(1-y)] + K_y$$

where n is the number of limitations of the intercalation process ($n=1$ or 2) (from an ionic or/and

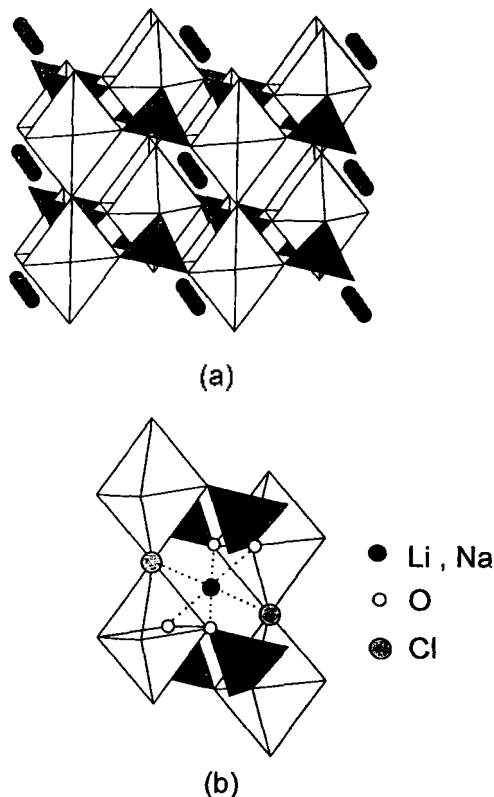


Fig. 6. Perspective view of the $AFeMoO_4Cl$ ($A=Li, Na$) structure (a) and the octahedral environment of lithium in $AFeMoO_4Cl$ (b).

electronic origin) and K reflects the interaction between the inserted species (ions and electrons) and the host lattice or the other inserted species. Various shapes of $V=f(y)$ curves are obtained depending on the value of K . They characterize the existence of a solid solution (continuous variation of V vs y) or of a two phase domain (potential plateau). In the latter case, Li^+ ions are intercalated as a result of the electrostatic attractive interaction with host, leading to a phase separation.

The OCV experiments, as shown in Fig. 7, have been carried out using $FeMoO_4Cl$ and $LiFeMoO_4Cl$ (chemically prepared) as the starting electrode materials. Those cells have been discharged and charged with relaxation periods, respectively. The electrode material has been considered as being in equilibrium (i.e. without concentration gradient within the grains) when the slope of voltage vs

time curve was smaller than 0.1 mV per hour (Fig. 7). The ideal open circuit voltage curve is represented by the continuous line as shown in Fig. 7b. As previously discussed, this behavior is characteristic of a biphased domain with a narrow solid solution in the vicinity of $x=1.0$.

The cells consisting of the chemically prepared material were electrochemically charged and discharged around the composition range of $x=1.0$, with relaxation periods till reaching to an equilibrium. The two curves are represented in Fig. 8. Their shapes show the existence of a solid solution around $x=1.0$ with biphased domains on both

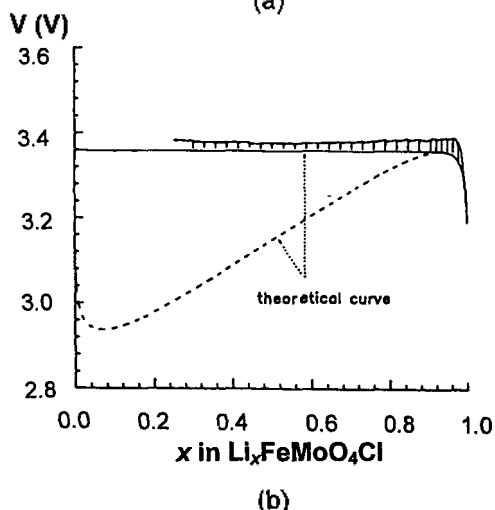
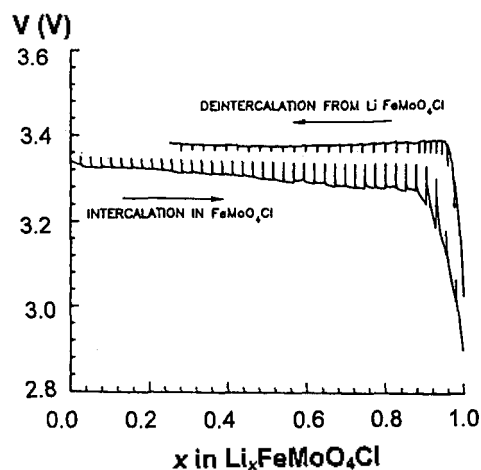


Fig. 7. Experimental (a) and theoretical (b) potentials vs composition curves for the $Li_x/FeMoO_4Cl$ cell.⁸

sides (the left one is the same as that reported in Fig. 7). The OCV values have been fitted using Armand's model. In the present case, y is equal to x , the amount of Li^+ intercalation.

From the results of magnetic study^{1,7} and the sample colors, it is thought that the electrons are localized (Fe^{3+} or Fe^{2+}) in both limiting phases. In the ionic point of view, all Li^+ sites are occupied for $x=1$. Therefore, n has been chosen as 2 because there are two limitations of the intercalation process for this system. The results of OCV curve fits are shown in Fig. 7b (dotted line) and Fig. 8. With the value of $K=0.8$, the best fitted results could be obtained for the first one denoted as (I) in Fig. 8. This K value characterizes strong electrostatic attractive interactions between Li^+ ions and host FeMoO_4Cl , leading to a very large biphased domain. In this respect, it could be assumed that the energies of the end member phases of FeMoO_4Cl and $\text{LiFeMoO}_4\text{Cl}$ are very different from one another, due to the electronic localization and the change of interlayer spacing. Therefore, at the beginning of the intercalation, the large value of K induces the topotactic germination and growth of the $\text{Li}_{x-1}\text{FeMoO}_4\text{Cl}$ phase.

The OCV curve shows the existence of a solid solution in the range of $0.95 \leq x \leq 1.06$. For higher

values of x , another biphased domain is observed, where the voltage plateau at 2.8 V is very narrow. Then the voltage drops rapidly to the following plateau at 1.7 V (Fig. 3). For $x > 1$, the electrochemical intercalation implies the reduction of hexavalent molybdenum to the pentavalent one. During this reaction, an amorphization of the material occurs as previously discussed. A biphased domain is therefore also expected.

The (II) curve shape in Fig. 8, corresponding to electrostatic repulsive interactions ($K \leq 0.204$), results from the beginning of occupancy for the second type of tunnels by Li^+ ions and from the reduction of hexavalent molybdenum. For higher intercalation amounts ($x > 1.06$) (curve (III) in Fig. 8), the structure becomes unstable and consequently a phase separation occurs. The curves (II) and (III) in Fig. 8 have not been fitted, but they were drawn in order to show the various domains.

The relation between the voltage of lithium and sodium cells and the structural dimensionality of the positive electrode material

The voltage plateau of Li and Na cells are equal to 3.36 and 3.08 V, respectively. This difference corresponds practically to that in potential between Li and Na electrodes in an absolute scale. When an intercalation process involves very strong electrostatic attractive interactions, leading to a broad biphased domain, the voltage plateau is fixed by the limiting lithium composition close to AFeMoO_4Cl ($A=\text{Li}$ and Na) in our case, where the voltage value is given by the maximum of the calculated curve as shown in Fig. 7b. Thus $\text{LiFeMoO}_4\text{Cl}$ and $\text{NaFeMoO}_4\text{Cl}$ (in fact the lower limit of the solid solution around the AFeMoO_4Cl composition) have approximately the same potential in an absolute scale. Due to the similarity of their electronic properties, it can be concluded that both materials have very close Madelung energies. A similar behavior has been found for several intercalation compounds with 3D framework structure like $\text{AFe}_2(\text{MoO}_4)_3$ ($A=\text{Li}$ and Na)¹¹ and $\text{A}_{1+x}\text{Ti}_2(\text{PO}_4)_3$.^{12,13} When the Li and Na cells were built with the $\text{AFe}_2(\text{MoO}_4)_3$ and $\text{A}_{1+x}\text{Ti}_2(\text{PO}_4)_3$ materials as positive electrodes, the cell voltage difference

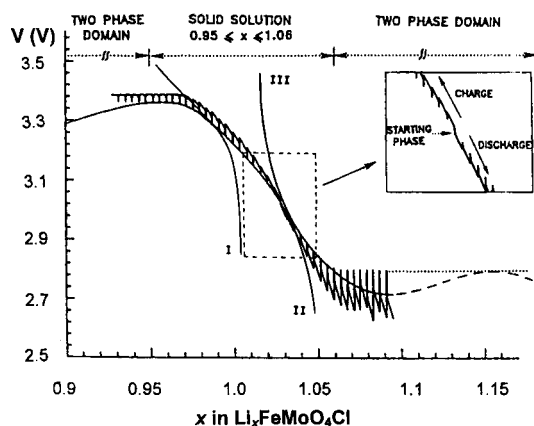


Fig. 8. Comparison between experimental and theoretical curves for the $\text{Li}/\text{FeMoO}_4\text{Cl}$ cell in the vicinity of the $\text{LiFeMoO}_4\text{Cl}$ composition. Two cells have been realized from the starting phase; one has been charged and the other has been discharged.

results exclusively from the contributions of the negative plates.

On the contrary, for the A_xMO_2 layer compounds, the difference in voltage between Li and Na cells is equal to about 1 V. This behavior has been attributed to a strong modification of the Fermi level position resulting from the Madelung energy modification due to the difference in interslab spacing between Li and Na layered phases.¹⁴⁻¹⁶

As a conclusion, the electrochemical behavior of the intercalates $LiFeMoO_4Cl$ and $NaFeMoO_4Cl$ can be correlated with their structure with 3D skeleton, in contrast to the 2D character of the pristine phase.

Acknowledgment. This work was in part supported by the Korea Science and Engineering Foundation through the Center for Molecular Catalysis, and by the Electronics and Telecommunications Research Institute.

REFERENCES

1. Choy, J. H.; Noh, D. Y.; Park, J. C.; Chang, S. H.; Delmas, C.; Hagemuller, P. *Mat. Res. Bull.* **1988**, *23*, 73.
2. Delmas, C.; Chang, S. H.; Noh, D. Y.; Choy, J. H. *Solid State Ionics* **1990**, *40/41*, 563.
3. Choy, J. H.; Park, N. G.; Yoon, J. B.; Han, K. S.; Chang, S. H. *Jpn. J. Appl. Phys.* **1997**, *36*, 2656.
4. Choy, J. H.; Yoon, J. B.; Park, N. G.; Kim, Y. I.; Han, K. S. *Jpn. J. Appl. Phys.*, **1997**, accepted.
5. Torardi, C. C.; Calabrese, J. C.; Lazar, K.; Rieff, W. M. *J. Solid State Chem.* **1984**, *51*, 376.
6. Torardi, C. C.; Rieff, W. M.; Lazar, K.; Zhang, J. E.; Cox, D. E. *J. Solid State Chem.* **1987**, *66*, 105.
7. Torardi, C. C.; Rieff, W. M.; Lazar, K.; Zhang, J. E.; Prince, E. *J. Phys. Chem. Solids* **1987**, *66*, 105.
8. Choy, J. H.; Noh, D. Y.; Chang, S. H.; Delmas, C. *Eur. J. Solid State Inorg. Chem.* **1990**, *27*, 391.
9. Choy, J. H.; Park, N. G.; Chang, S. H.; Park, H. H. *J. Kor. Chem. Soc.* **1995**, *39*, 446.
10. Armand, M. B.; In *Materials for Advanced Batteries*, Murphey, D. W.; Broadhead, J.; Steel, B. C. H., Ed.; NATO Conf. Series, Plenum Press: 1980; p 145.
11. Nadiri, A.; Delmas, C.; Salmon, R.; Hagemuller, P. *Rev. Chim. Min.* **1984**, *21*, 537.
12. Nadiri, A.; Delmas, C. *C. R. Acad. Sci.* **1987**, *C 304*, 415.
13. Delmas, C.; Cherkaoui, F.; Nadiri, A.; Hagemuller, P. *Mat. Res. Bull.* **1987**, *22*, 631.
14. Delmas, C.; Braconnier, J. J.; Maazaz, A.; Hagemuller, P. *Rev. Chim. Min.*, **1982**, *19*, 343.
15. Delmas, C. In *Chemical Physics of Intercalation*, Legrand, A. P.; Flandrois, S. Ed.; NATO ASI Series 1987; p 209.
16. Delmas, C. *Mat. Sci. Eng.* **1989**, *B3*, 97.